Analytical Methods

Accepted Manuscript

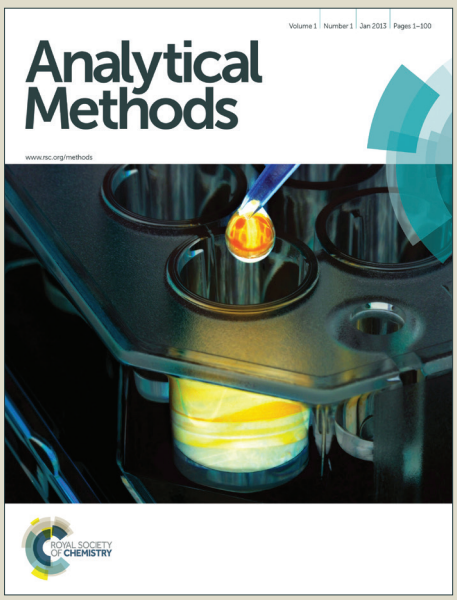

ROYAL SOCIETY OF CHEMISTRY

www.rsc.org/methods

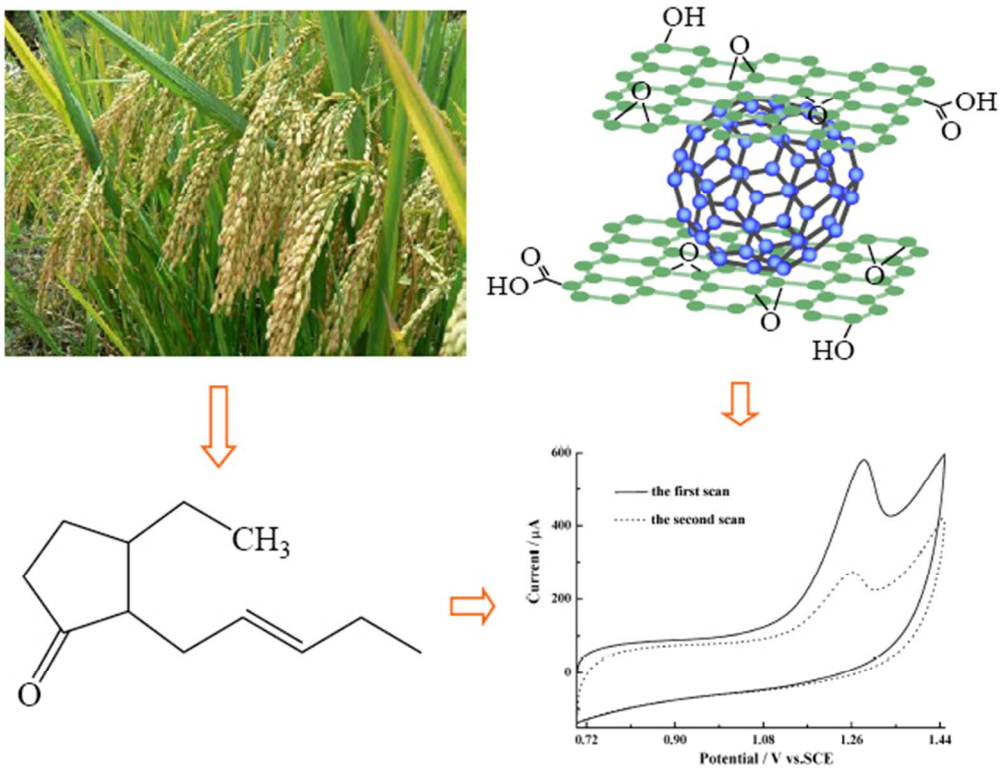

169x129mm (96 x 96 DPI)

Preparation of graphene oxide–fullerene/phosphotungstic acid films and their application as sensor for the determination of cis–jasmone

Tian Gan,[ac] Chengguo Hu,[bc] and Shengshui Hu[*bc]

Recent progress in nanotechnology has promoted research interest in surface functionalization of graphene oxide (GO) nanosheets for their large specific surface area and abundant functional groups. In the present work, cage structure of fullerene (C60) was noncovolent attached on the laminar GO through simple grinding, which not only achieved the efficient solubilization of C60 in water but also remained the original physicohemical characteristics of GO and C60. The C60–GO nanocomposite could be well dispersed in water with solubility up to 5 mg mL^{-1} and stability for more than one month. Further combining the redox reversibility of phosphotungstic acid (PTA), a novel electrochemical sensing film (PTA–C60–GO) was fabricated by one–step electropolymerization on pretreated home–made graphite electrode (GE). This PTA–C60–GO/GE exhibited a sensitive electrochemical response for the direct oxidation of *cis*–jasmone (CJ)，a well known component of plant volatiles. Under optimal conditions, the oxidation current of CJ linearly increased with its concentration in the range of 0.3~50.0 μmol L^{-1} with a detection limit of 0.1 μmol L^{-1}. This sensing platform has been applied to the determination of CJ content in rice spikelet samples.

1 Introduction

Many plants undergo a series of metabolic changes including the defensive chemicals and release of volatile

[a]*College of Chemistry and Chemical Engineering, Xinyang Normal University, Xinyang 464000, PR China*

[b]*College of Chemistry and Molecular Sciences, Wuhan University, Wuhan 430072, PR China. E–mail: sshu@whu.edu.cn; Fax: +86-27-68754067; Tel: +86-27-87881642*

[c]*State Key Laboratory of Transducer Technology, Chinese Academy of Sciences, Beijing 10080, PR China*.

organic compounds to protect themselves when attacked by herbivores. The end–products or intermediates of *α*–linolenic acid, such as jasmonic acid, methyl jasmonate, 12–oxophytodienoic acid have been verified to play prominent role as such volatile compounds to regulate the plant defence against herbivores.[1,2] Besides, *cis*–jasmone (CJ), a metabolite derived from the biosynthesis of jasmonic acid,[3] can also change the benzoxazinoid levels in crops and therefore reduce the aphid population.[4] Furthermore, CJ is directly attractive to the predacious seven–spot ladybird, in an olfactometer, and to the aphid parasitoid.[3] Thus, the development of a high sensitive method for the determination of CJ in crops is very important.

Unfortunately, only rare methods have been reported. M.H. Meshkatalsadat[5] and P. Guedes De Pinho[6] developed time–consuming gas chromatography/mass spectrometry for the analysis of volatile organic compounds including CJ. And two indirect electrochemical sensors have been fabricated in our previous work,[7,8] but with low sensitivity.

The research on fullerenes has induced a broad scientific interest in the areas of physics, chemistry and also materials science after their isolable production by Krätschmer et al.[9] As a special single molecule of fullerenes, C60 has a high electron affinity (ca. 2.7–2.8 eV) and its 30 carbon–carbon double bonds can act as radical sponge.[10] However, C60 forms aggregates in aqueous solutions and which restricts its biological applications seriously. Up to now, many covalent methods through cycloadditions[11] and nucleophilic additions[12] have been proposed. But an alternative nondestructive way for increasing the solubilization of C60 in polar solutions has attracted more attention, as observed for carbon nanotube[13] or graphene.[14] Recently, graphene–based materials have showed extraordinary electronic, thermal and mechanical properties and the potential of a variety of promising applications, especially in electrochemical sensors.[15] And as known to all, graphene oxide (GO) is a kind of hydrophilic material because of the large number of polar groups, such as hydroxyl, epoxide, ether, and carboxylate groups on the surface of the graphite layers.

In this work, laminar GO was bound to the C60 cages through π–stacking interaction by simple grinding and no

need for further separation. This not only increased the dispersibility of C60 but also hindered the aggregation of GO layers, and was expected to exert higher determination sensitivity than bare GO. The formed C60–GO hybrid can dispersed in water stably for several months. Further combining the redox reversibility of phosphotungstic acid (PTA), a strong solid acid which have been used as catalysts in several industrial processes and many promising reactions,[16] a novel sensing film was fabricated by one–step electropolymerization on pretreated home–made graphite electrode (GE). This electrochemical sensor based on PTA–C60–GO film exhibited high electrocatalytic activity and accumulation ability for the direct electrochemical oxidation of CJ with an apparently reduced oxidation overpotential and a much higher sensitivity. This electrochemical sensor has been applied to the determination of CJ in spikelet samples of rice.

2 Experimental procedures

2.1 Reagents and solutions

CJ and C60 were purchased from Aldrich, USA. Graphite (specpure), PTA and other chemicals were purchased from the Sinopharm Group Chemical Reagent Co., Ltd, China with analytical purity. All chemicals were used as received without further purification. The water used was re–distilled.

Fourier transform infrared spectroscopy (FTIR) spectra were obtained on a Magna–IR 550 system (Nicolet, USA). UV–vis absorption spectrum was performed on a UV–vis spectrophotometer (UV–2550, SHIMADZU). Fluorescence spectra were recorded by fluorescence spectrophotometer (RF–5301PC, SHIMADZU). The field emission scanning electron microscopy (FESEM) images were performed on a Sirion 200 field scanning electron microscope (FEI, Holland). Electrochemical measurements were carried out on a CHI 660B electrochemical workstation (Chenhua Instruments, China). A three electrode system using a PTA–C60–GO modified pretreated GE, a saturated calomel reference electrode (SCE) and a platinum wire counter electrode was used.

2.2 Synthesis of graphene oxide (GO)

GO was synthesized according to a modified Hummer's method[17] as follows. Firstly, the graphite was preoxidized by thermic concentrated H_2SO_4, $K_2S_2O_8$ and P_2O_5. Secondly, the preoxidized graphite was further oxidized with iced concentrated H_2SO_4 and $KMnO_4$. Lastly, yellow–brown GO could be obtained after being washed by 10% HCl solution and water for several times.

2.3 Noncovalent functionalization of C60 by GO

C60 was mixed with GO on a weight ratio of 1:3 in an agate mortar and ground for 2 h by hand with no others to add, producing a C60–GO colloidal powder with uniform color. Then, 50.0 mg of this powder was added into 10 mL water in a glass vial. The glass vial was allowed to be treated under ultrasonic environment with a frequency of 60 KHz for 2 h. The formed suspension of C60–GO is black–brown, apparently different from the yellow–brown suspension of GO with same concentration (Fig. 1A). No filtration or washing was needed in the whole process. And the possible bonding mode between laminar GO and cage–like C60 was shown in Fig. 1B.

2.4 One–step electropolymerization of PTA–C60–GO on pretreated graphite electrode

GE was home–made from the pencil leads (0.7 mm in diameter and comprise about 85.5 wt% graphite and 14.5 wt% clay, which were purchased from a local market) according to our previous work.[18] GE was anodized at +1.8 V for 240 s and then cathodized at –1.8 V for 240 s in 0.1 mol L^{-1} $HClO_4$. Thereafter, the GE was successively scanned between 1.2 and 1.8 V until stable cyclic voltammograms were obtained. The pretreated GE was rinsed by water for subsequent use.

Appropriate volume of the well dispersed C60–GO suspension was added into 40 mmol L^{-1} PTA aqueous solution to make the final concentration of C60–GO is 0.1 mg mL^{-1}. One–step electropolymerizaiton was

performed on GE in the PTA–C60–GO aqueous solution using cyclic voltammetry (CV) technique. The scan range is –0.95~0.25 V, the scan rate is 100 mV s^{-1}, and the scan cycles are 50. Finally, the PTA–C60–GO film modified GE was carefully rinsed with water and air dried, which was denoted to PTA–C60–GO/GE. The fabrication of PTA/GE or PTA–GO/GE was similar to the above procedures except that the electrolyte was replaced by 40 mmol L^{-1} PTA or 40 mmol L^{-1} PTA containing 0.1 mg mL^{-1} GO in water.

2.5 Analytical procedure

5.0 mL of 0.1 mol L^{-1} $HClO_4$ solution was added to the cell containing a specific amount of CJ. Unless stated otherwise, differential pulse voltammetry (DPV) began at 0.8 V after a 180 s accumulation. Pulse amplitude = 50 mV, pulse period = 200 ms. All experiments were conducted at room temperature.

3 Results and discussions

3.1 Characterizations

The FTIR spectra of GO and C60–GO samples are shown in Fig. 1C. The spectra of GO confirms the presence of C–O–H (ν_{O-H} at 3422 and 1367 cm^{-1}), COOH ($\nu_{C=O}$ at 1713 and 1428 cm^{-1}), C–O–C (ν_{C-O} at 1229 cm^{-1}). The band at 1636 cm^{-1} is due to the deformation of the O–H bond in water. The peaks locate at 1097 and 1059 cm^{-1} are due to C–O (i.e., hydroxyl, ether) stretching vibrations. The absorption bands below ~1000 cm^{-1} are due to the presence of trace sulfate groups by H_2SO_4 intercalated between graphite planes, or possibly as the free acid.[19] In the case of C60–GO, the peaks located at 1416, 1179, 578 and 526 cm^{-1} arise from the fundamental IR active internal modes for C60.[20] Besides, the main characteristic peaks of GO still exist and the positions of these peaks do not move with only difference in strength, indicating the noncovalent π–stacking between C60 and GO which keeps the initial structure of them perfectly.

Fig. 2A shows the UV–vis absorption spectra of C60–GO in water. The spectrum of C60–GO exhibits absorptions at 259 and 346 nm, which are characteristic of dissolved C60 in aqueous solution. The absorptions of GO at about 230 and 300 nm due to the π–π* transitions of C=C and n–π* transitions of C=O may overlap with the peaks of C60 at 259 and 346 nm. The broad absorption between 428 and 562 nm arises from close electronic interactions among adjacent C60 molecules is a feature of solid–state, crystalline C60. Therefore, C60–GO may be not dispersed in water molecularly, but is dispersed as fine solid clusters.[21] The emission spectra of C60–GO composite were recorded under irradiation by 250 nm in the range 300–435 nm as shown in Fig. 2B. It can be seen that the characteristic fluorescence emission of C60 at 369 nm in water is significantly quenched in C60–GO (i.e., measurements performed with matching absorbencies at the excitation wavelength).

The surface morphology of different electrodes was characterized by FESEM (Fig. 3). As expected, GE is composed of compact graphite sheets with sharp edges, and some amorphous impurities are attached on the graphite sheets (a). After the anodic treatment of the GE (b), it is found that the gaps between graphite sheets begin to disappear gradually, and the amorphous impurities almost disappear. The graphite sheets are more close to each other and the sharp edges of original graphite sheets can not be seen. Furthermore, the surface of the GE becomes very smooth except a few pieces can be observed after the GE was further cathodized (c). This may because the large graphite flakes are cut off under violent condition, and lots of very small pieces are formed. Interestingly, it is obvious that the anodized and cathodized treatments have serious influence on the surface morphology of GE, which can change the graphite sheets from micrometer–scale to nanometer–scale, eliminate the amorphous impurities among graphite layers and make the electrode surface more uniform and smooth. These changes are advantageous for subsequent electropolymerization of composite film evidently. When the PTA was solely electropolymerized on the GE surface (d), it can be seen that lots of round PTA particles coat densely on the electrode with diameters between 186 and 457 nm. The thickness of the PTA film can be regulated by changing the

scan cycles and scan rate during the electropolymerization. However, the shape of PTA crystals changed a lot after the GO (e) or C60–GO (f) was co–electropolymerized. The original stereoscopic PTA crystals are crushed to fracted crystals with the cotton–like appearance, this may be caused by the excellent affinity between the colloidal carbon film (i.e., GO or C60–GO) and the carbon electrode surface, and which proves the success of the one–step electropolymerization. Moreover, the GO film with folded structure is somewhat thick because the PTA crystals under it are blurry to see (e). This is due to the aggregation of GO layers. But after the insertion of C60 molecules, the GO layers are separated from each other. So the C60–GO composite film is very thin and owns favorable flexibility which can attach tightly on the PTA surface (f). In addition, it is evident that the PTA crystals on C60–GO composite film modified electrode are much denser.

The different film modified electrodes were characterized and compared by cyclic voltammetry (CV) (Fig. 4). It could be seen from curve a that the CV curve of untreated GE in 0.1 mol L^{-1} $HClO_4$ is very smooth with very low background current, and no evident redox peak can be seen. The similar condition can be obtained on cathodized GE, but the cyclic voltammetric background current has evident increase (curve b), implying the electrode surface area and double–layer capacitance increase, too.[22] Big difference can be observed after the modification of GE with PTA (curve c), PTA–GO (curve d) and PTA–C60–GO (curve e) that there are three couples of redox peaks in 0.1 mol L^{-1} $HClO_4$ obviously. These redox peaks can be attributed to the two 1–electron and one 2–electron redox processes of PTA.[23] This indicates that the electropolymeric films are firmly fixed on GE surface. Besides, the existence of GO and C60–GO not only maintains the redox properties of PTA, but also increases the electrode surface area with different degrees because the cyclic voltammetric background currents of PTA/GE, PTA–GO/GE and PTA–C60–GO/GE increase gradually.

3.2 Direct electrocatalytic oxidation of cis–jasmone

Fig. 5 depicts the DPV behaviors of 30.0 μmol L^{-1} CJ in 0.1 mol L^{-1} $HClO_4$ at different modified electrodes. There is only a very small oxidation peak (I_p = 1.70 μA) located at 1.46 V on GE (curve a). This oxidation peak has witnessed an increase (I_p = 12.37 μA) on the pretreated GE (curve b), and the oxidation peak potential shifts negatively (E_p = 1.37 V). As observed in the FESEM images, the GE surface becomes much smoother with nano–scale, and the impurities are removed after being pretreated, these are the reasons for the increase of peak current and the decrease of peak potential at pretreated GE compared to untreated GE. At PTA/GE, the oxidation peak current of CJ has an increase of about three times and the oxidation peak potential has an obvious negative shift (about 176 mV) (curve c), indicating the PTA crystals improve the surface area of GE largely and own strong catalytic effect on the electrochemical oxidation of CJ. When GO (curve d) or C60–GO (curve e) was co–electropolymerized on GE with PTA, the electrochemical signal of CJ improves significantly, exhibiting as the further increasing of the peak current and decreasing of the peak potential. It is interesting that the oxidation peak potential of CJ shifts negatively for almost 300 mV at PTA–C60–GO/GE compared with GE. In addition, the PTA–C60–GO/GE shows no evident peak in 0.1 mol L^{-1} $HClO_4$ solution (curve f), which confirms the attribution of the oxidation peak at 1.16 V to CJ. As discussed in the section 3.1, the good affinity between the GO or C60–GO film and the electrode surface can fix the PTA crystals to the electrode surface firmly and therefore exerts the catalytic ability of PTA to a large extent. Furthermore, the existence of these carbon films can greatly increase the surface area and accumulation capacity of the electrode. At the same time, C60 may be reduced partially during the electropolymeric process and then exhibits favorable conductivity as a kind of effective electron transfer medium, which makes C60–GO composite film more advantageous for the electron transfer compared to only GO film. Therefore, the C60–GO, together with PTA, show intensive catalytic effect for the direct electrochemical oxidation of CJ.

Fig. 6 depicts the successive CV behaviors of 0.2 mmol L^{-1} CJ in 0.1 mol L^{-1} $HClO_4$ at PTA–C60–GO/GE. There is a sensitive oxidation peak on the first scan from 0.7 V to 1.4 V, and no reduction peak appeares on the subsequent reverse scan, indicating the electrochemical oxidation of CJ is a totally irreversible process. On the second scan, the oxidation peak current of CJ decreases evidently, which may be caused by the adsorption of the oxidation product of CJ on the electrode surface. However, the PTA–C60–GO/GE could be renewed by continuous scan between 1.2 and 1.8 V in 0.1 mol L^{-1} $HClO_4$ for 20 cycles.

3.3 The effect of scan rate

The effect of scan rate (v, mV s^{-1}) on the electrochemical behavior of CJ was investigated by linear scan voltammetry (LSV). It was found that the oxidation peak current of CJ increased linearly with the increase of scan rate from 25 to 200 mV s^{-1}, showing that the oxidation of CJ is an adsorption–controlled electrochemical process. In addition, the oxidation peak potential (E_p, V) of CJ has a linear relationship with v according to the regression $E_p = 1.174 + 0.0561 \log v$ ($r^2 = 0.999$). Furthermore, according to Laviron's equation,[24] for an adsorption controlled and totally irreversible electrode process, E_p and v are defined by the following equation:

$$E_p = \frac{2.3RT}{\alpha n_\alpha F} \times \log\left(\frac{RTk_f^0}{\alpha n_\alpha F v}\right) \qquad (1)$$

where α is the transfer coefficient, n_α is the electron transfer number during the rate–determining step, and k_f^0 is the heterogeneous electron exchange rate constant. From Eq. 1, the value of αn_α can be calculated to be 1.05 from the slop (25 °C). Assuming that α is 0.5, so $n_\alpha = 2.11$ is obtained. Therefore, the oxidation of CJ is a two–electron irreversible electrochemical oxidation process.

3.4 Optimization of experimental conditions

The influence of different supporting electrolyte on the electrochemical response of CJ on PTA–C60–GO/GE was

studied. The electrolyte such as 0.1 mol L^{-1} Na_2HPO_4–NaH_2PO_4 buffer (pH 1.0~8.0), 0.2 mol L^{-1} NaAc–HAc buffer (pH 3.5~5.6), $Na_2B_4O_7$–HCl buffer (pH 9.2~12.3), 0.1 mol L^{-1} NaOH, HCl, H_2SO_4 and $HClO_4$ were included. The results showed that there is no oxidation peak of CJ appeared in alkaline environment at all, but an oxidation peak in neutral electrolyte, and the most well–defined oxidation peak in strong acidic solution like 0.1 mol L^{-1} HCl, H_2SO_4 and $HClO_4$. However, the biggest peak current and the best peak shape of CJ could be obtained in 0.1 mol L^{-1} $HClO_4$, so it was chosen as the determining electrolyte for CJ at PTA–C60–GO/GE system.

The potential range and scan cycles during electropolymerization were also optimized because they have direct influence on the thickness and surface morphology of the PTA–C60–GO film. When the initial potential for electropolymerization changed from –0.75 V to 1.15 V and the final potential changed from 0.05 V to 0.45 V, it was found that the electrochemical response of CJ was most sensitive on the PTA–C60–GO film electrode prepared between –0.95 and 0.25 V. Thus, the PTA–C60–GO film was electropolymerized on the GE surface by cycling in the range of –0.95~0.25 V.

The effect of electropolymeric cycles was then investigated. When the scan cycles were less than 50, the oxidation peak current was weak because the prepared PTA–C60–GO film was thin and incomplete, and the formed PTA crystals were small. However, the biggest electrochemical signal can be obtained after the GE was scanned in PTA–C60–GO aqueous solution for 50 cycles. If the scan cycles were more than 50, the PTA–C60–GO film would become too thick and which may hinder the electron transfer of CJ on the electrode surface. So the peak current of CJ showed a decrease. Therefore, 50 was chosen as the best electropolymeric cycles.

Accumulation has great effect on the electrochemical response of CJ. The effect of accumulation potential was investigated firstly. It was found that the oxidation peak current of CJ had almost no change when the accumulation potential positively shifted from 0.5 to 0.9 V. So the accumulation potential has no influence on the electrochemical behavior of CJ, and the initial potential (*i.e.*, 0.8 V) was selected as the accumulation potential for

convenience. But unlike the accumulation potential, accumulation time has significant influence. The peak current of CJ increased dramatically when the accumulation time extended from 0 to 240 s, and then no longer increased when the accumulation time further protracted. Take both sensitivity and efficiency into consideration, 240 s was selected as the accumulation time for the detection of CJ.

3.5 Selectivity, calibration and reproducibility

Under the optimized experimental conditions described above, the effects of some substances on the current response of 5.0 μmol L^{-1} CJ were evaluated (Table 1). A 500–fold concentration of glucose, sucrose, soluble starch, oleic acid, castor oil acid, 400–fold concentration of SO_4^{2-}, PO_4^{3-}, 60–fold of CO_3^{2-}, 50–fold concentration of Mg^{2+}, Fe^{3+}, 20–fold concentration of Ca^{2+}, Fe^{2+}, Cu^{2+}, and 2–fold concentration of I^-, Br^- have almost no influence on the current responses of 5.0 μmol L^{-1} CJ (error < 6%). In order to assure the application of this electrochemical system to real sample, the effects of other phytohormone on the determination of CJ were also investigated. It was found that 500–fold concentration of methyl dihydrojasmonate, 100–fold concentration of gibberellin, 50–fold concentration of indole–3–acetic acid, 10–fold concentration of abscisic acid, salicylic acid, and 5–fold concentration of methyl jasmonate have no influence on the determination of CJ. These results indicate that the selectivity of present method is satisfied for the quantification of CJ.

The linear range and detection limit for CJ were investigated using DPV. From Fig. 7, it was found that the oxidation peak current of CJ on PTA–C60–GO/GE (I_p, μA) was linear with its concentration (c, μmol L^{-1}) over the range from 0.3 to 50.0 μmol L^{-1} (inset A of Fig. 7). The linear regression equation is $I_p = -0.261+2.94\ c$, and the correlation coefficient (r^2) is 0.999, revealing good linearity. After 180 s accumulation, the detection limit was evaluated to be 0.1 μmol L^{-1} based on gradually decreasing the concentration of CJ in electrolyte (inset B of Fig. 7).

The reproducibility and reusability of PTA–C60–GO modified GE for the determination of CJ were investigated. Repetitive determinations of CJ were carried out in 0.1 mol L^{-1} $HClO_4$ containing 5.0 μmol L^{-1} CJ. The used PTA–C60–GO/GE could be easily regenerated by potential cycling between 1.2 and 1.8 V at a scan rate of 100 mV s^{-1} in blank solution. The relative standard deviation (RSD) of 3.3% for CJ was obtained at the same PTA–C60–GO/GE for ten replicate measurements. While at the unmodified GE, the RSD value for ten replicate measurements was 10.12% for 5.0 μmol L^{-1} CJ. These results suggest that the PTA–C60–GO film modified GE has a good reproducibility for the determination of CJ.

3.6 Application in rice spikelet sample analysis

In order to evaluate the practical application of this novel electrochemical sensor, it was applied for the detection of CJ in rice spikelet samples. And the extrapolation method was selected considering the extremely low content of CJ in plant.[25] The rice spikelet samples were obtained from Jiangxi Agricultural University, China. CJ was extracted by quantitative 80% freezing methanol. Briefly, several methanol extracts of the rice spikelet samples were spiked with known and increasing amounts of CJ standard solution, *i.e.*, 0.3, 1.0, 3.0, 5.0, 10.0, 30.0 and 50.0 μmol L^{-1}, and the DPV curves were recorded according to the optimized experimental conditions (Fig. 8), the characteristic CJ signal was found to increase with the amount of CJ spiked (inset of Fig. 8). Additional five calibration plots were carried out under the same working conditions with different CJ standard spiked. The concentration of CJ in the rice spikelet samples (c_0) can be obtained from the intercept of plot CJ peak current (I_p) vs. the concentration of CJ spiked (c_{CJ}) by extrapolation to the vertical axis at $I_p = 0$. The average c_0 value obtained from the six calibration graphs is 62.48 ng g^{-1} (RSD = 3.24%). And the recoveries were calculated between 99.04 and 104.92%, which implies a good reliability of this method for real samples analysis. Furthermore, the same rice spikelet samples were analyzed using high performance liquid chromatography (HPLC) method, and the resulting

c_0 value of 63.57 ng g^{-1} was obtained. The c_0 data from this electrochemical method and the HPLC method are in substantial agreement, indicating the practicability of this method for the determination of CJ in real samples.

4 Conclusion

To sum up, the direct oxidation of *cis*–jasmone (CJ) on the surface of PTA–C60–GO modified GE was studied here. And a novel electrochemical method was successfully developed for the determination of CJ. This novel analytical method possesses short analysis time, handling convenience and good accuracy. It was used in practical sample analysis, and the results consisted with the values that were obtained by HPLC.

Acknowledgements

The work was supported by the National Natural Science Foundation of China (Nos. 90817103, 31070885 and 61201091).

References

1 E. E. Farmer and C. A. Ryan, *Proc. Natl. Acad. Sci. U. S. A.*, 1990, **87**, 7713–7716.

2 Y. Chen and Z. L. Chen, *Anal. Methods*, 2013, **5**, 1733–1738.

3 M. A. Birkett, K. Chamberlain, A. J. Guerrieri, M. J. Martin, M. Matthes, J. A. Napier, J. Pettersson, J. A. Pickett, G. M. Poppy, E. M. Pow, B. J. Pye, L. E. Smart, G. H. Wadhams, L. J. Wadhams and C. M. Woodcock, *Proc. Natl. Acad. Sci. U. S. A.*, 2000, **97**, 9329–9334.

4 M. C. Moraes, M. A. Birkett, R. Gordon–Weeks, L. E. Smart, J. L. Martin, B. J. Pye, R. Bromilow and J. A. Pickett, *Phytochemistry*, 2008, **69**, 9–17.

5 M. H. Meshkatalsadat and Y. Shabaninejad, *Dig. J. Nanomater. Biostruct.*, 2011, **6**, 359–363.

6 P. Guedes De Pinho, R. F. Gonçalves, P. Valentão, D. M. Pereira, R. M. Seabra, P. B. Andrade and M. Sottomayor, *J. Pharm. Biomed. Anal.*, 2009, **49**, 674–685.

7 X. P. Dang, C. G. Hu, Z. L. Chen, S. F. Wang and S. S. Hu, *Electrochim. Acta*, 2012, **81**, 239–245.

8 X. P. Dang, C. G. Hu, D. Shen, Z. L. Chen and S. S. Hu, *J. Electroanal. Chem.*, 2011, **657**, 39–45.

9 W. Krätschmer, L. D. Lamb, K. Fostiropoulos and D. R. Huffman, *Nature*, 1990, **347**, 354–358.

10 R. I. Stefan–van Staden and R. G. Bokretsion, *Aanl. Methods*, 2012, **4**, 1492–1497.

11 R. A. J. Janssen, J. C. Hummelen and F. Wudl, *J. Am. Chem. Soc.*, 1995, **117**, 544–545.

12 W. J. K. Zang, J. K. Sprafke, M. Ma, E. Y. Tsui, S. A. Sydlik, G. C. Rutledge and T. M. Swager, *J. Am. Chem. Soc.*, 2009, **1**, 8446–8454.

13 C. G. Hu, Z. L. Chen, A. G. Shen, X. C. Shen, J. Li and S. S. Hu, *Carbon*, 2006, **44**, 428–434.

14 X. H. An, T. Simmons, R. Shah, C. Wolfe, K. M. Lewis, M. Washington, S. K. Nayak, S. Talapatra and S. Kar, *Nano Lett.*, 2010, **10**, 4295–4301.

15 T. Gan and S. S. Hu, *Microchim. Acta*, 2011, **175**, 1–19.

16 T. Gan, C. G. Hu, Z. L. Chen and S. S. Hu, *Electrochim. Acta*, 2011, **56**, 4512–4517.

17 T. S. Sreeprasad, A. K. Samal and T. Pradeep, *J. Phys. Chem. C*, 2009, **113**, 1727–1737.

18 T. Gan, C. G. Hu, Z. L. Chen and S. S. Hu, *Sens. Actuator B–Chem.*, 2010, **151**, 8–14.

19 Y. Y. Liang, D. Q. Wu, X. L. Feng and K. Müllen, *Adv. Mater.*, 2009, **21**, 1679–1683.

20 D. S. Bethune, G. Meijer, W. C. Tang, H. J. Rosen, W. G. Golden, H. Seki, C. A. Brown and M. S. de Vries, *Chem. Phys. Lett.*, 1991, **179**, 181–186.

21 J. D. Fortner, D. Y. Lyon, C. M. Sayes, A. M. Boyd, J. C. Falkner, E. M. Hotze, L. B. Alemany, Y. J. Tao, W. Guo, K. D. Ausman, V. L. Colvin and J. B. Hughes, *Environ. Sci. Technol.*, 2005, **39**, 4307–4316.

22 Z. F. Li, J. H. Chen, D. W. Pan, W. Y. Tao, L. H. Nie and S. Z. Yao, *Electrochim. Acta*, 2006, **51**, 4255–4261.

23 J. Y. Liu, L. Cheng, B. F. Liu and S. J. Dong, *Electroanalysis*, 2001, **13**, 993–998.

24 E. Laviron, *Electroanal. Chem. Inter. Electrochem.*, 1974, **52**, 355–393.

25 T. Gan, C. G. Hu, Z. L. Chen and S. S. Hu, *J. Agric. Food Chem.*, 2010, **58**, 8942–8947.

Figure captions

Fig. 1 A: Photos of 5.0 mg mL^{-1} GO and C60–GO in water. B: Schematic represation of the sandwish–type C60 between two layers of graphene via π–stacking interaction. C: FTIR spectra of GO and C60–GO.

Fig. 2 A: UV–vis absorption spectrum of C60–GO. B: The fluorescence emission spectra of GO and C60–GO. All the spectra were recorded in water and against the solvent as reference.

Fig. 3 FESEM images of GE (a), anodized GE (b), cathodized GE (c), PTA/GE (d), PTA–GO/GE (e) and PTA–C60–GO/GE (f).

Fig. 4 Cyclic voltammograms of CE (a), cathodized GE (b), PTA/GE (c), PTA–GO/GE (d) and PTA–C60–GO/GE (e) in 0.1 mol L^{-1} $HClO_4$. Scan rate: 100 mV s^{-1}.

Fig. 5 DPV behaviors of 30.0 μmol L^{-1} CJ at GE (a), cathodized GE (b), PTA/GE (c), PTA–GO/GE (d) and PTA–C60–GO/GE (e) in 0.1 mol L^{-1} $HClO_4$. Curve f corresponds to DP voltammogram of PTA–C60–GO/GE in blank. Accumulation time: 180 s; pulse amplitude: 50 mV, pulse period: 200 ms.

Fig. 6 Successive cyclic voltammograms of 0.2 mmol L^{-1} CJ in 0.1 mol L^{-1} $HClO_4$ at PTA–C60–GO/GE. Scan rate: 100 mV s^{-1}.

Fig. 7 DPV curves at PTA–C60–GO/GE for various concentrations of CJ including 0.3, 1.0, 3.0, 5.0, 10.0, 30.0

and 50.0 μmol L^{-1} (from inner to outer). Inset A: the calibration graph. Inset B: the DP voltammogram of PTA–C60–GO/GE in blank (a) and in 0.1 μmol L^{-1} CJ (b). Other conditions are as in Fig. 5.

Fig. 8 DP voltammograms obtained in rice spikelet samples spiked with 3.0, 5.0, 8.0, 10.0, 30.0 and 40.0 μmol L^{-1} CJ from inner to outer in 0.1 mol L^{-1} $HClO_4$. Inset: calibration graph using extrapolation method. DPV conditions are as in Fig. 5.

Table 1 The influence of some interferents on the peak current of 5.0 μmol L^{-1} CJ

Interferents	Concentration (μmol L^{-1})	Signal change (%)
Methyl dihydrojasmonate	2500.0	3.21
Gibberellin	500.0	–5.03
Indole–3–acetic acid	250.0	–3.42
Abscisic acid	50.0	–3.99
Salicylic acid	50.0	5.83
Methyl jasmonate	25.0	–4.58
Glucose	2500.0	1.47
Sucrose	2500.0	–1.55
Soluble starch	2500.0	2.44
Oleic acid	2500.0	2.35
Castor oil acid	2500.0	1.86
SO_4^{2-}	2000.0	–3.74
PO_4^{3-}	2000.0	–2.16
CO_3^{2-}	300.0	–4.64
Mg^{2+}	250.0	3.25
Fe^{3+}	250.0	3.02
Ca^{2+}	100.0	4.09
Fe^{2+}	100.0	3.23
Cu^{2+}	100.0	6.04
I^-	10.0	–5.28
Br^-	10.0	–5.76

Fig. 1

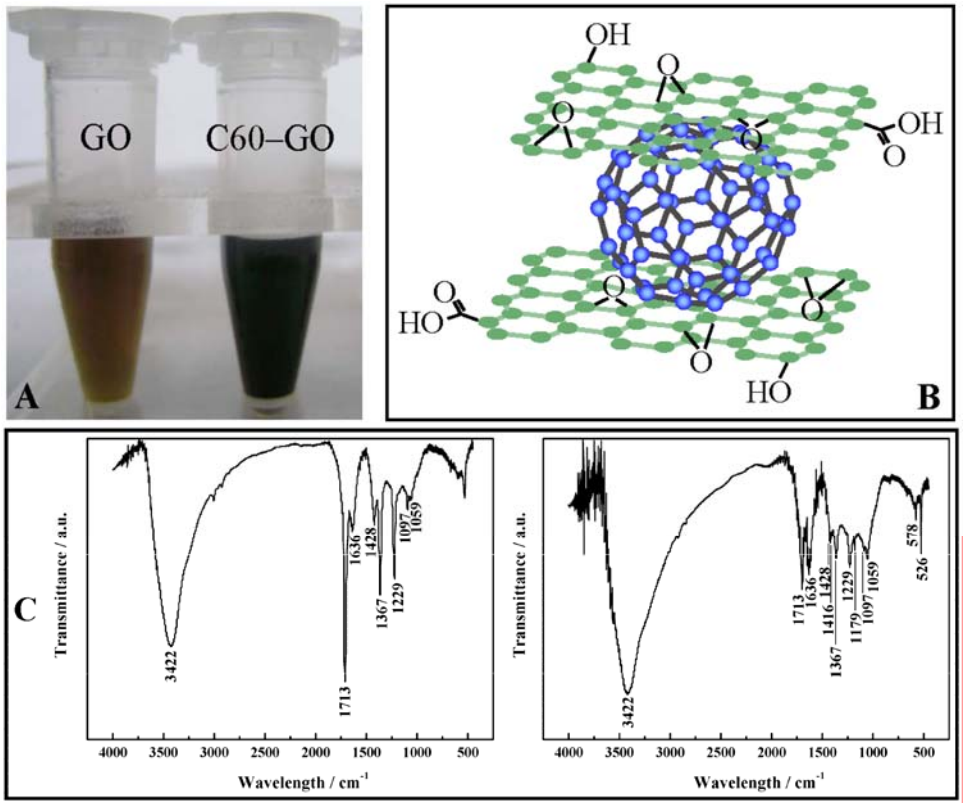

Fig. 2

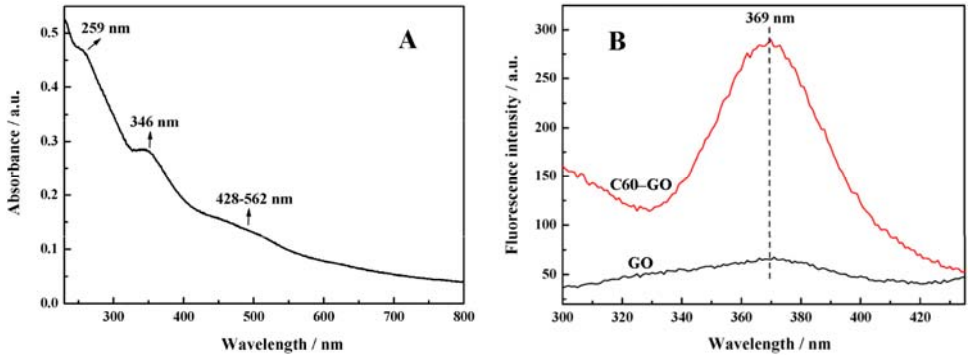

Fig. 3

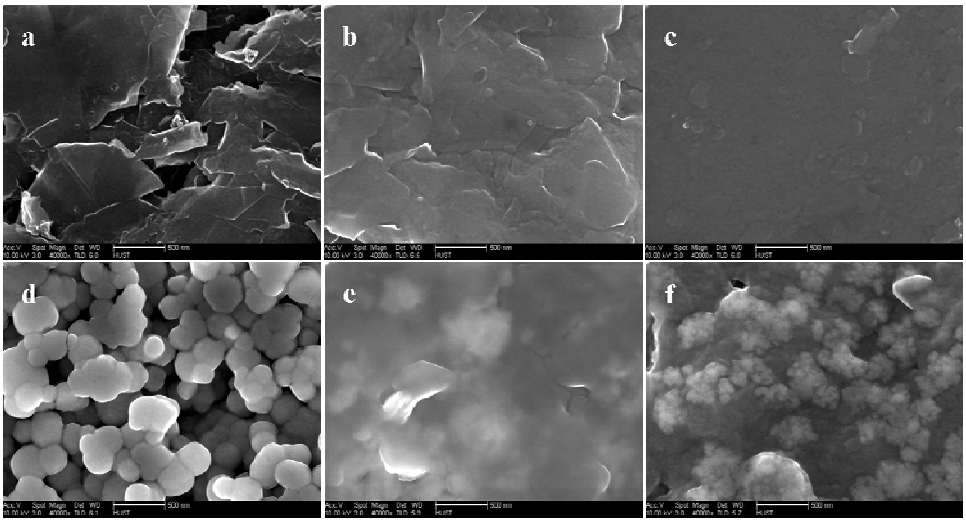

Fig. 4

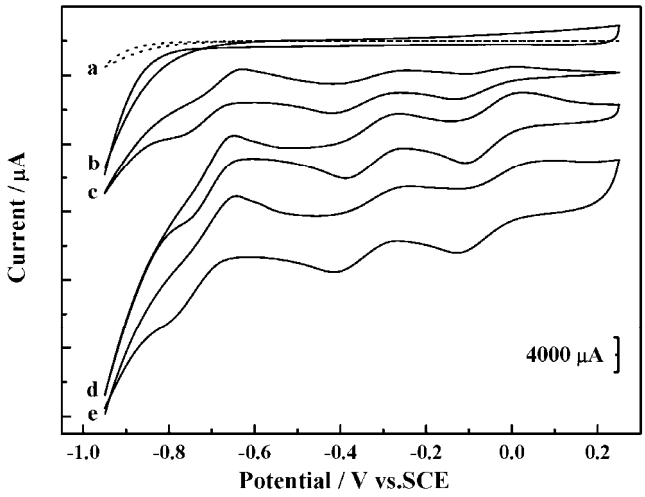

Fig. 5

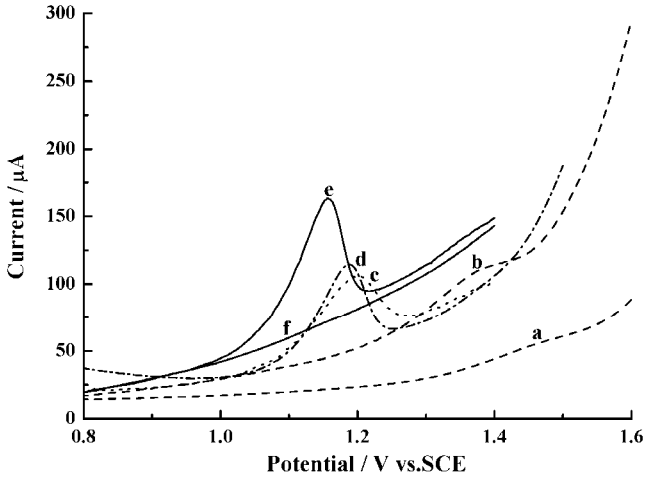

Fig. 6

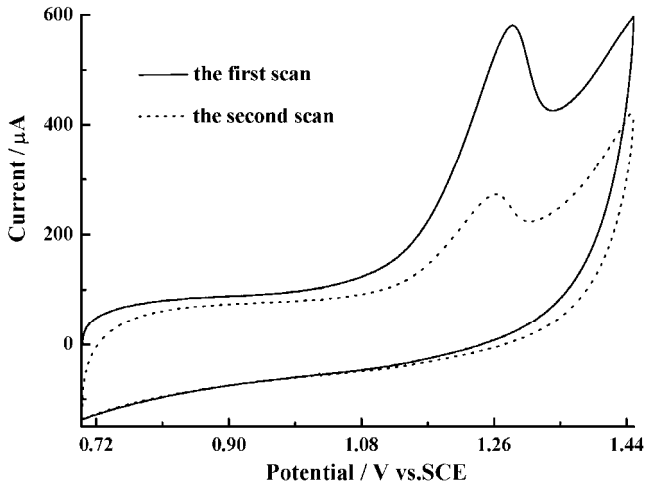

Fig. 7

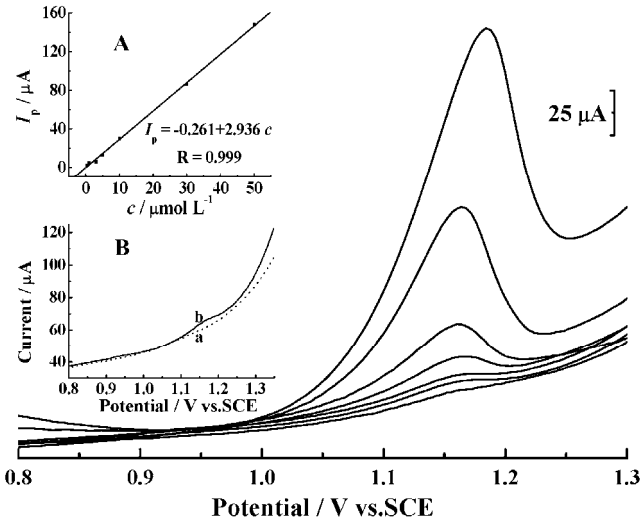

Fig. 8